THE JOURNAL OF PHYSICAL CHEMISTRY B

ARTICLE

pubs.acs.org/JPCB

Ca L_{23} Spectrum in Amorphous and Crystalline Phases of Calcium Carbonate

Peter Rez* and Alexander Blackwell

Department of Physics, Arizona State University, Tempe, Arizona, 85287-1504 United States

Supporting Information

ABSTRACT: The calcium L_{23} absorption edge is very sensitive to changes in local symmetry. Distinct spectra from calcite and aragonite as well as two different amorphous phases of calcium carbonate have been reported. Multiplet calculations using the CTM4XAS code, taking account of the local symmetry and the crystal field, suggest that the coordination octahedra are distorted by a change in length along one axis, the reduction in symmetry being coupled with tetrahedral displacements of the 4 atoms in the perpendicular plane. Examination of the polarization dependence implies that the two different amorphous phases arise from different levels of ordering of the oxygen coordination polyhedra around calcium. The change in the ordering suggests a pathway for the transformation to single crystal calcite. Although the code is unable to directly simulate the very low symmetry environment of Ca in aragonite, some degree of agreement is obtained with the same distortion of the coordination octahedron and greater tetrahedral displacements.

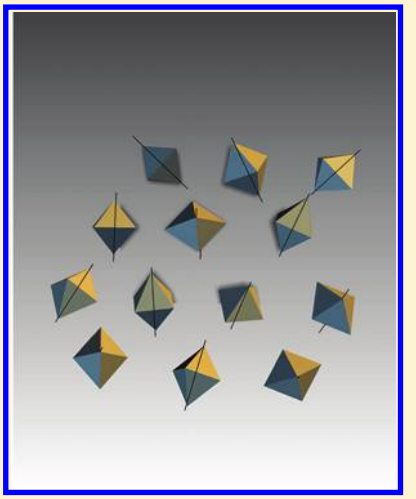

INTRODUCTION

Biogenic amorphous calcium carbonate (ACC) that subsequently transformed to calcite was first identified in the sea urchin spine.[1] Later work showed amorphous calcium carbonate precursors in other species, such as Acsidian spines[2] and more recently in the earthworm's calciferous gland.[3] A summary of observations of biogenic ACC is given by Weiner.[4] Amorphous calcium carbonate can also be synthesized in the laboratory by reacting $CaCl_2$ and a Na_2CO_3 solution at high pH.[5] Some ACC phases (strictly should be called polymorphs) transform rapidly to calcite, whereas others are stable for extended periods. Both the magnesium and water content vary among biogenic amorphous calcium carbonate phases[6] with up to 45% (atomic) Mg being observed in the sea urchin tooth.[7] Some ACC has water content similar to monohydrocalcite, whereas others are believed to be anhydrous. Recent work has suggested that prenucleation clusters of calcium and carbonate ions are the first stage in the formation of biogenic calcite.[8,9] These aggregate as ACC, before undergoing solid-state transformations that eventually result in single crystal calcite.

The atomic structure of the amorphous phase and the transformation mechanisms to calcite are still poorly understood. Pair distribution functions extracted from X-ray diffraction of synthetic ACC show a lack of structural coherence beyond 1.5 nm,[10] whereas Ca K edge EXAFS for both synthetic and biogenic ACC show a 6 fold coordination of O around Ca, similar to calcite,[11] though there is 25% uncertainty in this estimate. NMR indicates that the hydrogen signal arises from water molecules not hydrogencarbonate.[10,12] The most prominent physical features of ACC are the lack of optical birefringence and the reduction in ratio of the $\nu 4$ to $\nu 2$ IR absorption peaks[13] from the ratio observed in calcite.

When recorded at high energy resolution, approximately 0.1 eV, the Ca L_{23} edge shows distinctive features for calcite and two different amorphous phases. Using these fingerprint spectra X-ray photoelectron spectromicroscopy (X-PEEM) has recently been used to map the transformation in the sea urchin larval spicule,[14,15] and the sea urchin tooth.[16] The calcite spectrum shows 4 distinct peaks corresponding to the crystal field split L_3 and L_2 lines. One of the amorphous phases, labeled type 1, is observed in the early stages of the transformation and is believed to be hydrated. The Ca L_{23} lines show only two peaks with shoulders. The other phase, labeled type 2, shows two peaks on the higher energy L_2 line but only one on the lower energy L_3 line. It represents the later stages of the transformation and is believed to be anhydrous. Spectra from aragonite are similar to those from the type 1 amorphous phase, except that the peak on the low energy side of the L_3 line is hardly visible and the peak on the low energy side of the L_2 line has much reduced intensity.[17−19] Experimental spectra[14,17] showing these trends are presented in

Received: April 1, 2011
Revised: August 22, 2011
Published: August 23, 2011

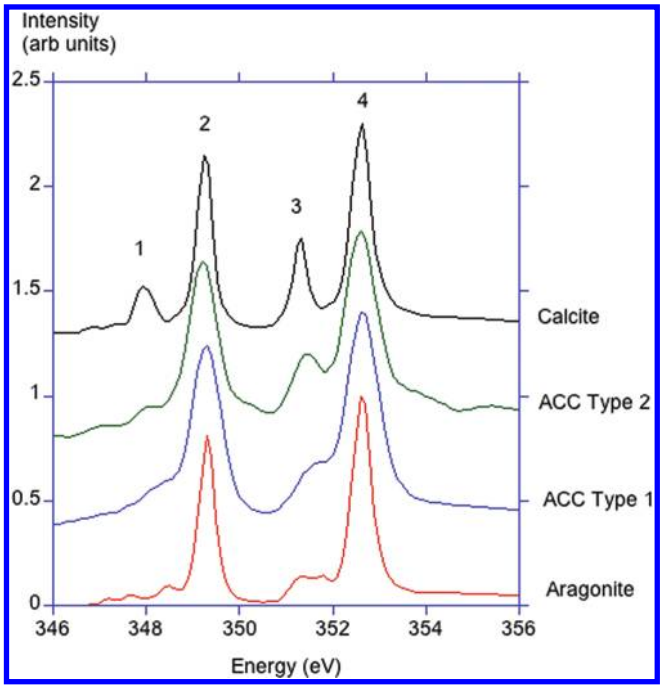

Figure 1. Experimental Ca L_{23} spectra from calcite, the two different ACC phases and aragonite[14,17].

Figure 1. The aragonite and calcite spectra were recorded from geologic specimens, the two different ACC spectra came from sea urchin embryo (Strongylocentrotus purpuratus) spicules that did not contain magnesium (P.U.P.A. Gilbert, private communication)

These spectra have still not been interpreted in terms of the atomic structure of the amorphous phases and any insights these might provide on a transformation mechanism.

In calcite the Ca ions are very close to being octahedrally coordinated by oxygen atoms. The Ca L_{23} edge is very sensitive to the symmetry of this coordination polyhedron. The changes can be studied theoretically by considering both the change in symmetry and the strength of a particular interaction. These have all been implemented in the CTM4XAS code originally developed by Thole[20] and extended by de Groot.[21] We show that the features observed in the spectra from the amorphous phases can be explained by distortions in the coordination polyhedron around the Ca ion and the disorder in the orientation of the coordination polyhedra in what eventually becomes the (0001) calcite plane.

The change to aragonite marks an extreme breakdown in symmetry at the calcium atom site to a single mirror plane. A measure of the breakdown in symmetry is the range of angles between Ca O bonds and the spread in bond distances. Matching the experimental spectra from the ACC phases with the results from simulations shows that the symmetry breakdown is not as severe as in aragonite. This imposes another constraint on bond angle distributions in candidate models for the ACC structure.

THEORY

As reported by de Groot et al.[22] and Himpsel et al.,[23] the fine structure of the Ca L_{23} lines in X-ray absorption or electron energy loss spectra is dominated by atomic multiplet effects that are then influenced by the local symmetry of the environment of

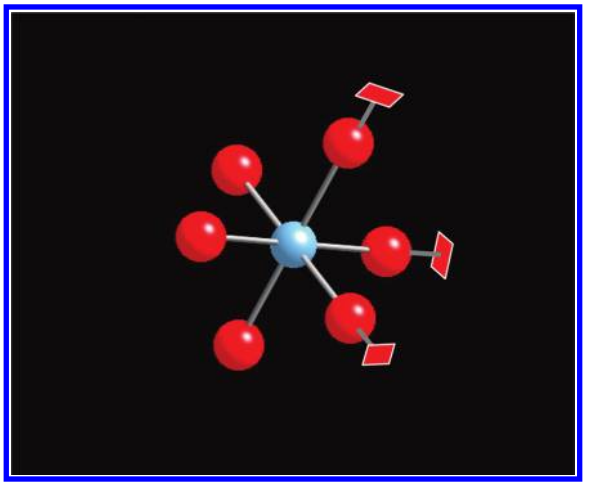

Figure 2. Coordination of Ca by O in calcite.

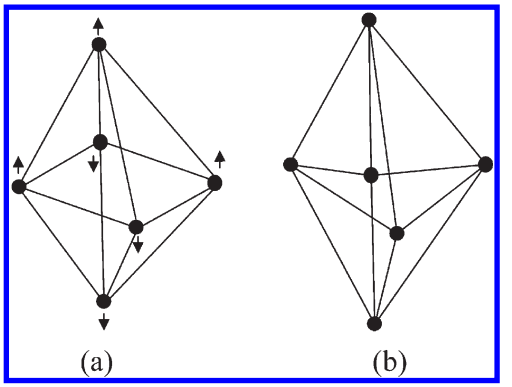

Figure 3. Distortion of the coordination polyhedron.

the particular ion. The L_{23} lines are the result of transitions of a 2p electron to an empty 3d state. A simple analysis would suggest that there are two lines, one from the $2p_{3/2}$ state labeled L_3 and the other from the $2p_{1/2}$ state labeled L_2. In calcite, space group $R\bar{3}c$, the coordination of Ca by the 6 nearest neighbor oxygen atoms is close to being octahedral, as shown in Figure 2. Published structures[24,25] show a stretching along what would be a 111 direction if the ligands were aligned along the *x*, *y*, and *z* axes. The angles between Ca−O bonds are either 87.25° or 92.75° rather than the 90° that would be observed with perfect octahedral coordination. In the absence of this slight distortion this symmetry would be denoted by O_h in Schoenflies notation and the 2 lines each split into 2 levels, from the molecular orbitals e_g and t_{2g}.

A more rigorous analysis recognizes that the 2p spin orbit coupling is large and that the total angular momentum $J = L + S$ is the relevant quantum number. The overall symmetry of the initial state with no d electrons is $^1S_0$, $J = 0$. The selection rules for the final state is $\Delta J = 1$ so there are three final states $^1P_1$ $^3P_1$ and $^3D_1$, which, in principle, gives rise to three lines. One, however is very weak, and appears as a small peak on the low energy side of the L_3 peak. Group theory is then used to determine what happens in octahedral symmetry. The initial state has group label A1, and the final state has label T1. Projecting the atomic states on to the octahedral group states shows that there now must be seven lines. The three lowest energy lines are very weak and give rise to structure on the low energy side of the first peak.

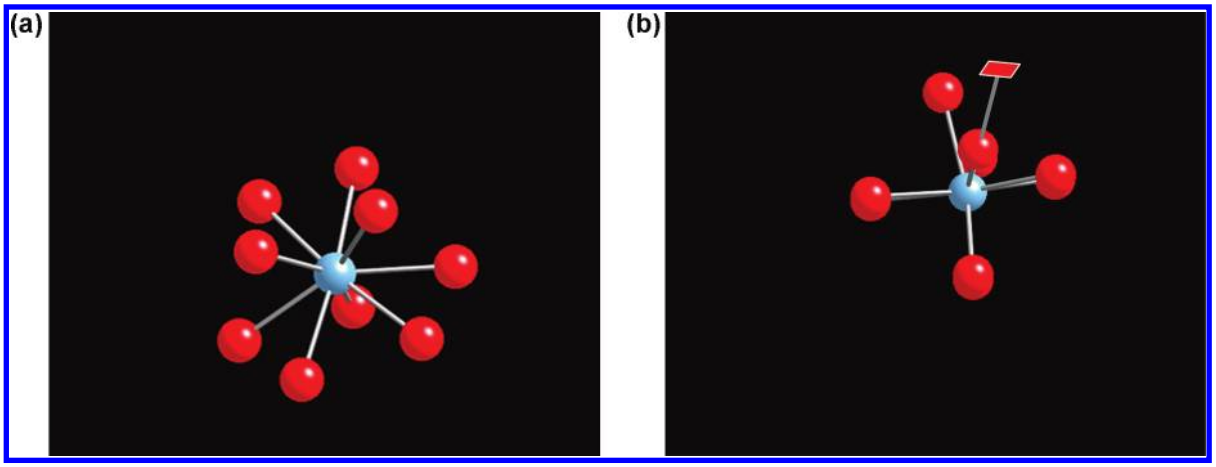

Figure 4. (a) Coordination of Ca by O in aragonite. (b) View showing approximate 4-fold symmetry down [200].

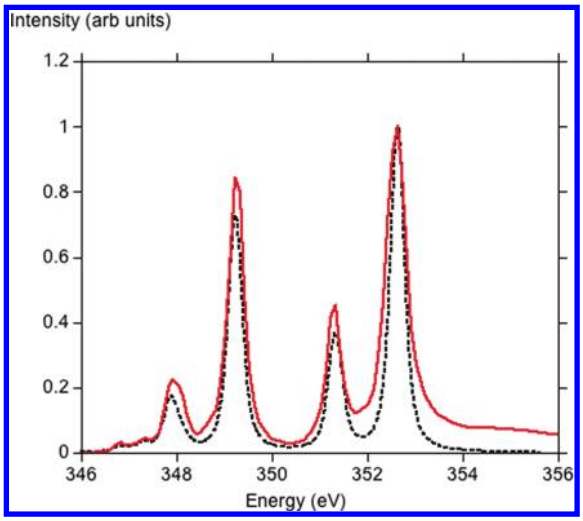

Figure 5. Comparison between simulated (dashed line) and experimental (solid line) spectrum of Ca $L_{2,3}$ lines in calcite.

(see Figure 5) The other four lines are the L_3 and L_2 peaks, each split into peaks that can be attributed to transitions to the t_{2g} and e_g levels of the simple model mentioned above. The magnitude of the splitting is controlled by the octahedral crystal field parameter, 10 Dq.

Lower symmetry involves distorting the coordination polyhedron of oxygen around the Ca ions. The two oxygen atoms on the z axis in Figure 1 could be moved further from the Ca ion, reducing the overally symmetry to tetragonal or 4 fold symmetry. Displacing the atoms in the $x-y$ plane as shown in the Figure 3 gives a small tetrahedral distortion. The consequences of these displacements and reductions in local symmetry are best studied using the CTM4XAS code (we used version 3α). The code starts with the atomic multiplets from a transition element ion, first projects these states to O_h, and then to one of two lower tetrahedral symmetries, D_{4h} or C_{4v}. Octahedral crystal fields are still represented by 10 Dq, with another parameter representing the strength of the tetrahedral crystal field. The resulting spectrum lines can then be convoluted with a Lorentzian to match intrinsic broadening and a Gaussian for experimental broadening.

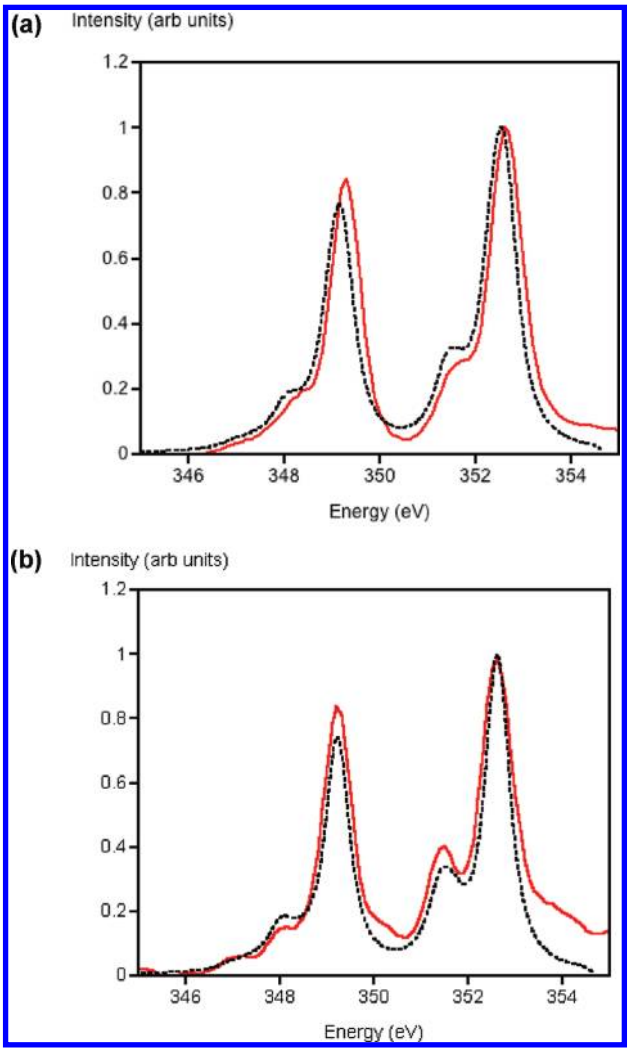

Figure 6. (a) Comparison of simulation (dashed line) with experiment (solid line) for type 1 ACC. Average over all directions of polarization, and a tetrahedral crystal field of 0.05 eV. (b) Comparison of simulation-(dashed line) with experiment (solid line) for type 2 ACC. Average over all polarization directions in the $x-y$ plane (see Figure 3), and a tetrahedral crystal field of 0.05 eV.

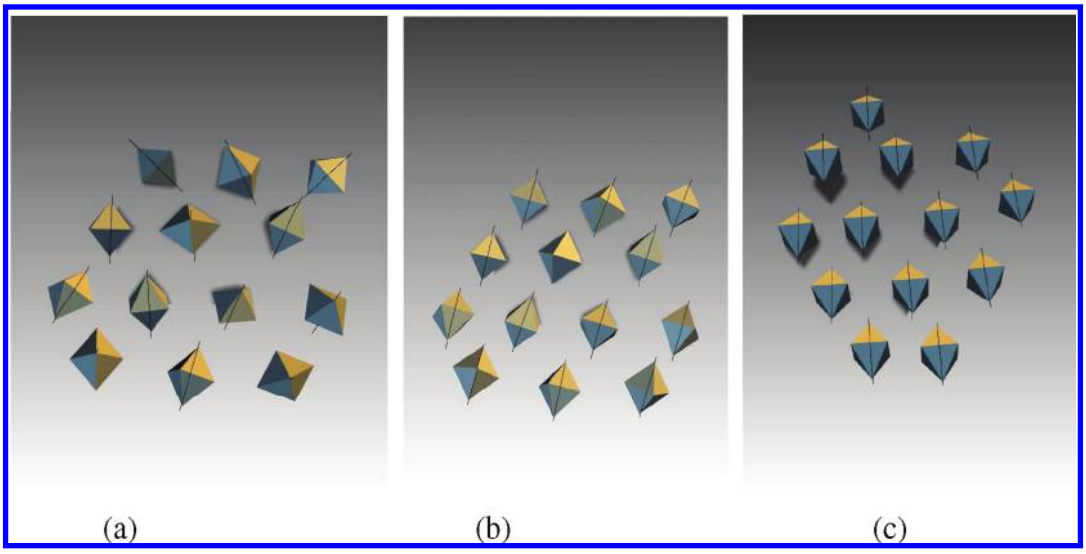

Figure 7. Arrangement of coordination polyhedra for (a) type 1 ACC, (b) type 2 ACC, and (c) calcite.

To match the experimental, spectra the octahedral crystal field parameter, 10Dq, was varied to best match the peak positions. Then the tetradrehral crystal field parameter, Dt, and the square field parameter, Ds, were systematically varied over a range of 0−1.2 eV and a tableau of spectra generated as shown in Supporting Information, Figure S1. The tetrahedral parameter Dt was varied in smaller steps of 0.01 eV when it became apparent that the best fits were achieved with Dt = 0.1 eV and Ds = 0.0 eV, as shown in Figure S2. At this stage the Lorentzian or intrinsic width was also varied to match the experimental ACC spectra. Calculated spectra were also shifted in energy to match the experimental data.

The environment around the Ca ion in aragonite has even lower symmetry. The aragonite structure can be generated from calcite by stretching along the [11−21] direction. The unit cell is then orthorhombic,[26] space group Pmcn, containing eight formula units. The symmetry around the Ca atoms is significantly reduced and is now just a single mirror plane or C_{1h} in the Schoenflies notation, as shown in Figure 4. To evaluate the effects on the Ca L_{23} lines the symmetry should be reduced in successive stages, $O_h > D_{4h} > C_{4h} > C_{2h} > C_{1\,h}$. In this process the e_g line splits into two lines and the t_{2g} line splits into three lines. This group theory argument on its own does not explain the differences between the structure observed on the L_3 and L_2 peaks. The effects of tetrahedral distortions clearly also have to be taken into account. As an approximation we just consider the first stage of symmetry reduction, the reduction to tetragonal symmetry from the stretching of the coordination polyhedron.

RESULTS AND DISCUSSION

We obtain the best match to the calcite spectrum with a 10 Dq parameter of 1.15 eV, an intrinsic Lorentzian peak width of 0.1 eV, and an instrumental Gaussian broadening of a further 0.1 eV, as shown in Figure 5. The increased width of the L_3 peak compared to the L_2 peak is due to the extra decay channels from Coster−Kronig Auger decays. The quality of the agreement suggests that the small distortion from perfect octahedral symmetry resulting in O−Ca−O bond angles that differ from 90° does not have much effect.

In the X-PEEM from the larva spicule Politi et al.[14] showed two types of spectra from amorphous calcium carbonate. The first type was very similar to spectra from synthetic ACC where both peaks that they labeled 2 and 4 were suppressed. In the second type only the peak on the L_2 edge, labeled peak 2, was suppressed. We have managed to simulate both of these spectra with a tetrahedral crystal field of 0.05 eV and an increased intrinsic width of 0.265 eV, as shown in Figure 6, panels a and b. The reduction in symmetry to tetragonal means that the Ca −O bonds along the x−y axes are no longer equivalent to the Ca−O bond along the z axis.

The first type of ACC spectrum shown as Figure 6a corresponds to an average of polarization over all directions suggesting a random orientation of the coordination octahedra as shown in Figure 7a. The second type of spectrum shown as Figure 6b corresponds to an averaging of the polarization vector in the x−y plane perpendicular to the Ca−O bonds of different length that define the tetragonal axis. The geometry for acquisition of these X-PEEM images and spectra is similar to that used in the measurements of individual crystals in aragonite.[17] The X-ray beam impinges on the sample at a glancing angle of 16° and the polarization vector is almost perpendicular to the sample surface. The spicules are oriented along the crystallographic a and symmetry related directions at 120° from each other.[1] The type 2 phase is an intermediate between the type 1 phase and calcite. The calcite structure can be described in terms of planes of aligned coordination polyhedra. A model for the amorphous structure consistent with the spectrum would have the distorted octahedral aligned as in calcite, but rotated at random angles about the long Ca−O bonds defining the tetragonal axis (Figure 7, panels a and b). This model is also consistent with the conclusion that secondary nucleation is responsible for co orientation of the calcite crystals in the sea urchin tooth.[7]

In aragonite the symmetry breaking around the Ca ion is even more severe and can not be fully simulated with the CTMXAS code. The best match is with a tetrahedral crystal field of 0.1 eV and symmetry reduction to D_{4h} or C_{4v}, with an average over all possible angles between the polarization direction and the tetragonal symmetry axis as shown in Figure 8, panels a or b. The environment around Ca in aragonite only approximately

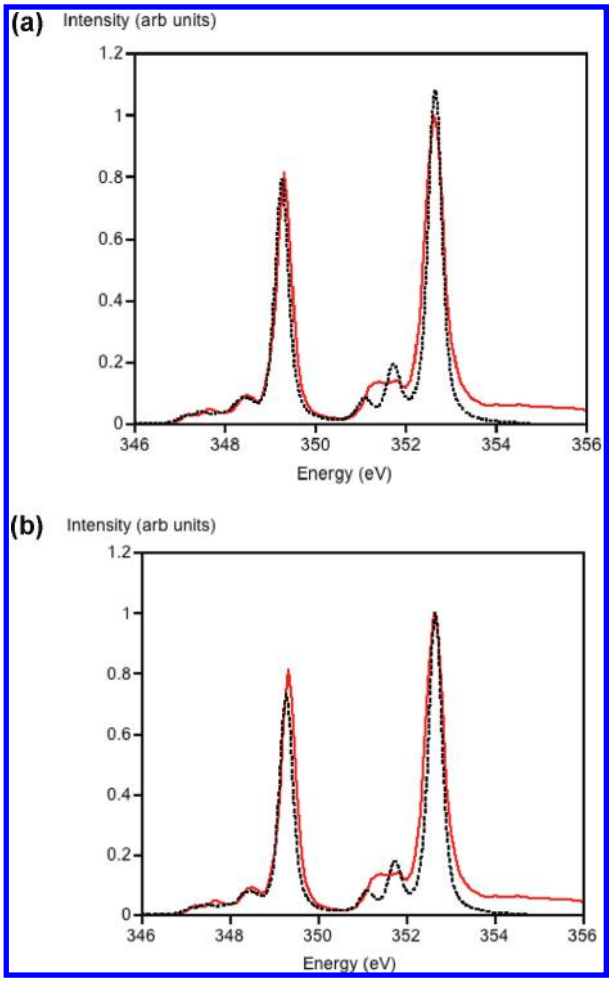

Figure 8. Comparison of simulation (dashed line) and measurement (solid line) for Ca L_{23} lines in aragonite in environment (a) D_{4h} and (b) C_{4v}. In both cases the tetrahedral crystal field was 0.1 eV.

matches a stretched octahedron with tetrahedral displacements of atoms in the $x-y$ plane (see Figure 4b). The first problem is that there are nine rather than six neighboring calcium atoms, which means that the coordinating polyhedron is no longer an octahedron. When viewed down [100] there is an approximate 4-fold symmetry which is possibly why the spectrum can even be approximately simulated with atom displacements of a distorted octahedron, though it should come as no surprise that the agreement is not perfect. The group theory analysis mentioned above, without the crystal field effects, would suggest that in D_{4h} or C_{4v} the t_{2g} only splits into two rather than the three lines that are observed.

From the smaller value of the tetrahedral field needed to simulate the ACC spectra compared with that needed to simulate the aragonite spectrum, it would appear that the symmetry breaking around the Ca site is not as severe. One way to characterize the symmetry breaking is to measure the angles between the lone bond in the mirror plane and the eight other Ca−O bonds (see Figure 3). The angles range from 72° to 145°, and the bond distances range from 0.242 to 0.265 nm (mean 0.2528, standard deviation 0.0085 nm), as shown in Table 1. This is in contrast to calcite, where the bonds are all almost 90° or 180° to each other, and the bond lengths are equal. It would be expected that in ACC the O−Ca−O angles span a somewhat smaller range than in aragonite.

Table 1. Aragonite Bond Lengths and Angles[a]

bond angle (degrees)	bond length (nm)
	0.242
144.6	0.245
93.6	0.252
81.3	0.255
71.9	0.265

[a] From ref 26.

The spectra suggest that the structure of ACC can be described in terms of randomly oriented distorted octahedra and that in the type 2 intermediate ACC phase there is alignment along the axis of compression or expansion. Given that other work has shown that the carbonate groups remain relatively undistorted, the structure is probably best described in terms of random carbonate tilts, which would be consistent with both the IR data and the loss of birefringence.

CONCLUSIONS

The Ca L_{23} lines are very sensitive to small changes in the coordination of neighboring oxygen ions. Experimental spectra from ACC can be matched by assuming the coordination polyhedra are stretched or compressed to give a 4-fold symmetry. There are also displacements of oxygen atoms in plane perpendicular to this axis that follow a tetrahedral symmetry. For ACC we achieved a best match with a tetrahedral crystal field splitting of 0.05 eV. Analysis of the polarization dependence of the spectra suggested that the 4-fold symmetry axis of the coordination octahedral is randomly oriented in the early stage type 1 ACC, and becomes aligned in the later stage type 2 ACC. The match between calculation and observation for aragonite is not as good since it was not possible to simulate the very low symmetry environment for Ca in aragonite using the code that was available to us. This probably is why the simulations show two peaks on the L_2 line while the observations and group theory predict three peaks. A tetrahedral crystal field of 0.1 eV gave the best fit which suggests that the range of O−Ca−O bond angles is not as large in ACC as in aragonite where it spans 70°. This acts as an additional constraint on any models for the atomic arrangements of ACC. High resolution X-ray spectroscopy of the Ca L_{23} lines gives important information about local coordination of Ca in biominerals. Simulation using multiplet codes such as CTM4XAS is a very powerful tool for extracting information about distortions in coordination polyhedra At present it is limited to two tetrahedral symmetries that do not encompass the full range of local Ca environments. Although agreement with experimental measurement for transition element L_{23} lines is very impressive one could argue that it is not a true first principles method since the Slater integrals are reduced by 20% and the ligand fields are not calculated from an electronic structure code. It is to be hoped that CTMXAS will be extended to the full range of local point groups in the near future.

ASSOCIATED CONTENT

Supporting Information. Figure S1 is a tableau showing the effects of varying the tetrahedral crystal field parameter, Dt, and the square distortion parameter, Ds, in steps of 0.1 eV up to 0.3 eV. Figure S2 shows the effects of varying the tetrahedral crystal field parameter, Dt, in steps of 0.01 eV up to 0.08 eV.

Table S3 summarizes the parameters used to model spectra for ACC, calcite and aragonite. This material is available free of charge via the Internet at http://pubs.acs.org.

AUTHOR INFORMATION

Corresponding Author
*E-mail: Peter.Rez@asu.edu.

ACKNOWLEDGMENT

P.R. thanks the Weizmann Institute of Science for awarding a Rosi and Max Varon visiting professorship. We also thank Prof J. B. Page for his careful review of group theory, Dr. F. M. F. de Groot for making available the CTM4XAS code, Prof P. U. P. A. Gilbert and Dr. Y. Politi for allowing us to use their experimental spectra, Mr. Jon Mull for help with the figures, and Profs S. Weiner and Lia Addadi for many stimulating discussions.

REFERENCES

(1) Beniash, E.; Aizenberg, J.; Addadi, L.; Weiner, S. *Proc. R. Soc. London B* **1997**, *264*, 461–465.
(2) Aizenberg, J.; Lambert., G.; Weiner, S.; Addadi, L. *J. Am. Chem. Soc.* **2002**, *124*, 32–39.
(3) Gago-Duport, L.; Briones, M. J. I.; Rodriguez, J. B.; Covelo, B. *J. Struct. Biol.* **2008**, *162*, 422–435.
(4) Weiner, S.; Levi-Kalisman, Y.; Addadi, L. *Conn. Tiss. Res.* **2003**, *44* (Suppl. 1), 214–218.
(5) Koga, N.; Nakagoe, Y.; Tanaka, H. *Thermochim. Acta* **1998**, *318*, 239–244.
(6) Raz, S.; Weiner, S.; Addadi, L. *Adv. Mater.* **2000**, *12*, 38–41.
(7) Killian, C. E.; Metzler, R. A.; Gong, Y. U. T.; Olson, I. C.; Aizenberg, J.; Politi, Y.; Wilt, F. H.; Scholl, A.; Young, A.; Doran, A.; Kunz, M.; Tamura, N.; Coppersmith, S. N.; Gilbert, P. U. P. A. *J. Am. Chem. Soc.* **2009**, *131*, 18404–18409.
(8) Gebauer, D.; Volkel, A.; Colfen, H. *Science* **2008**, *322*, 1819–1822.
(9) Pouget, E. M.; Bomans, P. H. H.; Goos, J. A. C. M.; Frederik, P. M.; se Wirth, G.; Sommerdijk, N. A. J. M. *Science* **2009**, *323*, 1455–1458.
(10) Michel, F. M.; MacDonald, J.; Feng, J.; Phillips, B. L.; Ehm, L.; Tarabrella, C.; Parise, J. B.; Reeder, R. J. *Chem. Mater.* **2008**, 1420–1428.
(11) Levi-Kalisman, Y.; Raz, S.; Weiner, S.; Addadi, L.; Sagi, I. *Adv. Funct. Mater.* **2002**, *12*, 43–48.
(12) Nebel, H.; Neumann, M.; Mayer, C.; Epple, M. *Inorg. Chem.* **2008**, *47*, 7874–7879.
(13) Raz, S.; Hamilton, P. C.; Wilt, F. H.; Weiner, S.; Addadi, L. *Adv. Funct. Mater.* **2003**, *13*, 480–486.
(14) Politi, Y.; Metzler, R. A.; Abrecht, M.; Gilbert, B.; Wilt, F. H.; Sagi, I.; Addadi, L.; Weiner, S.; Gilbert, P. U. P. A. *Proc. Natl. Acad. Sci.* **2008**, *105*, 17362–17366.
(15) Politi, Y.; Arad, T.; Klein, E.; Weiner, S.; Addadi, L. *Science* **2004**, *306*, 1161–1164.
(16) Ma, Y.; Aichmayer., B.; Paris, O.; Fratzl, P.; Meiborn, A.; Metzler, R. A.; Politi, Y.; Addadi, L.; Gilbert, P. U. P. A.; Weiner, S. *Proc. Natl. Acad. Sci.* **2009**, *106*, 6048–6053.
(17) Metzler, R. A.; Zhou, D.; Abrecht, M.; Chiou, J.-W.; Guo, J.; Ariosa, D.; Coppersmith, S. N.; Gilbert, P. U. P. A. *Phys. Rev. B* **2008**, *77*, 064110.
(18) Hahan, S.; Smith, A. M.; Obst, M.; Hitchcock, A. P. *J. Elect. Spectr.* **2009**, *173*, 44–49.
(19) Obst, M.; Dynes, J. J.; Lawrence, J. R.; Swehone, G. D. W.; Benzerara, K.; Karunakaran, C.; Kaznatcheev, K.; Tyliszcak, T.; Hitchcock, A. P. *Geochim Cosmochim. Acta* **2009**, *73*, 4180–4198.
(20) Thole, B. T.; van der Laan, G.; Fuggle, J. C.; Sawatzky, G. A.; Karnatak, R. C.; Esteva, J.-M. *Phys. Rev. B* **1985**, *32*, 5107–5118.
(21) de Groot, F. M. F. *Coord. Chem. Rev.* **2005**, *249*, 31–63.
(22) de Groot, F. M. F.; Fuggle, J. C.; Thole, B. T.; Sawatzky, G. A. *Phys. Rev. B* **1990**, *41*, 928–937.
(23) Himpsel., F. J.; Karlson, U. O.; McLean, A. B.; Terminello, L. J.; De Groot, F. M. F.; Abbate, M.; Fuggle, J. C.; Yarmoff, J. A.; Thole, B. T.; Sawatzky, G. A. *Phys. Rev. B* **1991**, *43*, 6899–6907.
(24) Graf, D. L. *Am. Mineral.* **1961**, *41*, 1283–1316.
(25) Markgraf, S. A.; Reeder, R. J. *Am. Mineral.* **1985**, *70*, 590–600.
(26) de Villiers, J. P. R. *Am. Mineral.* **1971**, *56*, 758–767.